

IMPROVEMENT OF THE BALANCE BETWEEN A REDUCED STRESS SHIELDING AND BONE INGROWTH BY BIOACTIVE COATINGS ONTO POROUS TITANIUM SUBSTRATES

Cristina Domínguez-Trujillo¹, Fátima Ternero¹, José Antonio Rodríguez-Ortiz¹, Juan José Pavón², Isabel Montealegre-Meléndez¹, Cristina Arévalo¹, Francisco García-Moreno³ and Yadir Torres^{1*}

¹ *Departamento de Ingeniería y Ciencia de los Materiales y del Transporte, Escuela Técnica Superior de Ingeniería y Escuela Politécnica Superior, Universidad de Sevilla, Sevilla, España*

² *Group of Advanced Biomaterials and Regenerative Medicine, Universidad de Antioquia, Bioengineering Program - Medellín, Colombia*

³ *Helmholtz-Zentrum Berlin für Materialien und Energie, Berlin, Germany*

* corresponding author: Y. Torres; ytorres@us.es; Escuela Técnica Superior de Ingeniería, Camino de los descubrimientos s/n, 41092 Sevilla, Spain; +34 954482278

ABSTRACT

Commercial pure titanium is known as good substitute for cortical bone tissue. Nevertheless, stress-shielding and the lack of osseointegration are still some limitations to solve. In this study, porous titanium substrates were manufactured by space-holder technique (50 vol% of NH_4HCO_3 with particle size between 250 and 355 μm). The obtained stiffness and yield strength of specimens were compatible with cortical bone tissue. The substrates were coated with three layers of Bioglass® 45S5 (BG) by dripping sedimentation, a new and economic technique. The porosity and surface characterization were performed by Archimedes' method,

image analysis, X-ray micro computed tomography and confocal laser microscopy, while the mechanical behavior was analyzed by ultrasound technique, uniaxial compression and micro-mechanical testing. Homogeneity, infiltration efficiency and coating integrity were evaluated. The adhesion of the coating was better on porous titanium substrates than on full dense ones. Finally, the bioactivity of the BG coating was determined via immersion in Simulated Body Fluid. The formation and growth of hydroxyapatite on the substrate were studied by scanning electron microscopy and X-ray diffraction analysis. The results showed hydroxyapatite formation in both coated full dense and porous samples. These features indicate the improvement of osseointegration for this sort of load bearing Ti implants.

Keywords: Porous titanium, stress shielding, Bioglass® coating, hydroxyapatite, in vitro bioactivity.

1. INTRODUCTION

Tissue degradation is considered one of the most important public health problems. Bone replacement via implants is a common solution to improve the life quality of patients. Its good functionality depends on intrinsic properties of the employed materials, quality and quantity of host tissue and the biointerface between implant and bone (surface energy, biochemistry and topography) [1]. Also, the related mechanical stimulation, the effects of some drugs and the systemic immunological influence are other important physical factors in implant behavior. Although titanium and Ti6Al4V alloy are frequently employed in bone replacement [2], they still present two problems to be solved: stress-shielding and poor osseointegration [3]. The fabrication of porous materials can reduce the difference of the Young's modulus between implant and bone [4]; and the osseointegration can be improved using bioactive coatings [5,6]. Bioactive glasses present adequate osteoconductivity and promote bone regeneration, controlling their biodegradability and forming bone mineral-like phases (hydroxyapatite, HA) [7]. Sol-gel, electrophoretic deposition, enameling, laser cladding, thermal spraying or thin film technologies are the most common techniques used to prepare bioactive glass coatings [2]. Nevertheless, their employment implies a high cost and an accurate control of several process parameters, as well as a detailed study of the coating bioactivity.

The micromechanical characterization, as well as biocompatibility of porous coatings on full dense titanium substrates have been studied by the scientific community [8,9]. However, no studies of porous titanium substrates have been reported. In these terms, the micro-computational tomography (micro-CT) is a useful tool for the microstructural substrates characterization [10]. It is a non-destructive method and allows obtaining very reliable quantitative and qualitative information [7-9]. This technique was proposed to study the trabecular bone architecture [11,12] and in bone tissue engineering applications [7,9]. In

addition, it is widely used in bone growth through the porous implant [4,13]. The main objective of this work is to manufacture BG-coated porous titanium substrates, which guarantee a better biomechanical and biofunctional balance.

2. MATERIALS AND EXPERIMENTAL PROCEDURE

Commercial pure (c.p.) porous titanium substrates were fabricated by the space-holder technique. Titanium grade IV powder was mixed with ammonium bicarbonate particles (NH_4HCO_3 , 50 vol% and particle size of 250-355 μm) in a turbula for 40 min. The blend was pressed at 800 MPa using an Instron 5505 universal testing machine. The space holder was removed in a furnace in 2 steps: 12 h (60 °C) and 12 h (110 °C). Both stages were performed in low vacuum conditions ($\sim 10^{-2}$ mbar). Then, the compacts were sintered in a Carbolyte® STF furnace (1250 °C, 2h at $\sim 10^{-5}$ mbar) and the substrates (full dense and porous Titanium) were coated with tri-layers of Bioglass® 45S5 (SCHOTT Vitryxx®) by using a new and economic deposition technique (sedimentation by dripping). The BG suspension was 10 mg/ml in ethanol [11]. Once the suspension was well stirred, 1 ml was distributed drop by drop onto the substrates, to be deposited in a homogeneous way. Finally, the samples were dried to evaporate the ethanol (one day per coating layer) before the final thermal treatment (TT), performed in a molybdenum furnace (820 °C, during 5 s at $\sim 10^{-5}$ mbar).

The microstructural characterization (total and interconnected porosity, P_T and P_i respectively) of substrates was performed by Archimedes' method [14], measuring five values of Archimedes' density in titanium substrates. Optical microscope (from Nikon Epiphot, Japan) coupled with a Jenoptik Progres C3 camera and analysis software Image-Pro Plus 6.2 was employed [15]. The tomography study was carried out by a custom-made X-ray scanner composed by micro focus X-ray source L8121-01 (with a W-target) operated at 100 kV and 100 μA , 5 μm , and a flat panel detector C7943 (120 mm \times 120 mm, 2240 \times 2368 pixel) (both

equipment from Hamamatsu, Japan). 3D volume of the specimen can be obtained acquiring a certain number of X-ray projections during sample rotation over 360°. Then, software reconstruction of these projections was used. This method allows the qualitative and quantitative evaluation of the inner structure of the porous Ti specimens. It has a spatial resolution down to 6.4 µm pixel size at a 7.8-fold magnification, in terms of pore size distributions, porosity, pore surface roughness, etc. [16].

The mechanical behavior was evaluated via: uniaxial compression test (stiffness and yield strength, E_c and σ_y respectively) according to ASTM E9-09 using a Instron 5505 universal testing machine [17,18]; ultrasound technique (dynamic Young's modulus, E_d), performed with a KRAUTKRAMER USM 35 equipment [19,20]; and Vickers micro-indentation (HV0.3 and HV1), ten measures per load and substrate.

Furthermore, surface roughness, structural integrity, homogeneity, infiltration grade and bioactivity of the coatings were studied. For that purpose, confocal laser microscopy, scanning electron microscopy (SEM) [21] and instrumented micro-indentation (P-h curves at 1 N load; Oliver and Pharr analysis) were used [22-24]. Two P-h curves were obtained for each BG-titanium system. Finally, the coated substrates were immersed in 50 ml of Simulated Body Fluid (SBF) at 37 °C in an incubator for 21 days, refreshing the solution every 14 days. The samples were rinsed (distilled water and absolute ethanol) and dried at 45 °C during 10 min. The bioactivity (formation and growth of HA) of the coated titanium substrates was analyzed by X-ray diffraction (XRD - Cu K α radiation to evaluate the crystalline phases formed), SEM (morphological features [9]) and energy dispersive X-ray spectroscopy (EDX - chemical composition). Five measures of Ca/P relation were carried out.

3. RESULTS AND DISCUSSION

The microstructural parameters and the micro-mechanical behavior of dense and porous titanium substrates are shown in Table I. Two different porosities are evaluated: the micro-porosity inherent to the sintering process (dense titanium) and the macro-porosity associated to the space holder. In terms of total porosity, the values obtained by all the analysis are lower than expected. The reasons could be: a) a small spacer amount could remain into the substrates, and/or b) a contraction of pores during the sintering process. The equivalent diameter (D_{eq}) of pores obtained via Image Analysis (IA) and micro-CT, agrees with the range of the particle sizes of NH_4HCO_3 . Comparing values, micro-CT total porosity and equivalent diameter are slightly smaller than the values measured by IA and Archimedes' method. The mechanical behavior in porous substrates depends on the obtained macro-porosity (greater size and pore fraction). Manufactured porous titanium substrates reduce the mismatch between the properties of cortical bone ($E= 20-25$ GPa and $\sigma_y = 150-180$ MPa) and the implant (see in Table I). The results of the micro-hardness depend on the applied indentation load. Otherwise, micro-hardness values for full dense substrate show higher values for HV0.3 (377 ± 39) than for HV1 (342 ± 16). This fact could be related to localized plasticity phenomena and the indentation size effects. The micro-hardness of porous substrate decreases due to the influence of the pores compared to full dense specimens. However, in both substrates (dense and porous) the values are similar for HV0.3, due to matrix remaining between the pores is "sufficiently large" to have a similar behavior to full dense substrate.

Figure 1 shows the pores size and morphology by different analysis techniques. Figure 1a) presents the different types of porosities explained above. The image of the micro-CT, Figure 1b), reveals the homogeneity of the pores distribution and different colours show the segmented and separated pores, being the Ti matrix transparent [25]. Moreover, the SEM images display, Figures 1c) and d), exhibit the roughness inside the pores. This topography enhances the osseointegration, promoting the cells adhesion according to previous works of

the authors [4,13]. The distribution of equivalent pore diameters and the corresponding Gauss fit is observed in Figure 2a) [26]. The mean equivalent pore diameter is 240 μm , which is in agreement with the range of the spacer particle size (250-355 μm). The Full Width at Half Maximum (FWHM) is 97.7 μm . A narrow distribution is observed. Figure 2b) depicts the distribution of the roughness volume percentage based on the relation of the pore volume to the eroded, smoothed volume of the same pore analyzed quantitatively from the tomographies as reported by Yin et al. [25]. It is observed that the relative roughness of the specimens decreases with increasing equivalent radius.

Figure 3 presents the macroscopic aspect of the substrates surfaces, before and after thermal treatment of the coating. The adhesion of the BG is clearly better for porous titanium than for dense substrate, since the anchoring effect is more effective due to interconnected pores and roughness in their walls [13]. The presence of chipping (poor adhesion) in some areas of dense substrate explains the increase of its surface roughness comparing to porous one. The presence of BG in the pores could promote the growth of HA inside them.

Figure 4 shows the 3D topography of un-coated and coated substrates. The images confirm the integrity of the coating and the infiltration of the BG into the pores (Figure 4 d)), as well as the morphology (porous) and the roughness on the coating.

The P-h curves are presented in Figure 5 [22-24], comparing the different coating-substrate systems with the pressed BG pellet. Coated porous titanium substrate presents a greater penetration depth (40 μm) than coated dense titanium substrate (37 μm) and sintered BG sample (12 μm). The presence of microporosity in the coating with BG, as well as the effect of the interface and the porosity of the substrate, could explain the lower rigidity and the hardness of the coating/substrate system. Regarding coated dense titanium substrate curve, a small fall or saw tooth is observed, that can be attributed to a lower adhesion of the coating to the substrate. In addition, a pseudo-creep behavior is observed. The presence of micro pores

in the BG may be the cause. XRD patterns confirmed that 45S5 Bioglass® powder is amorphous (state of supply), but once the powders were heat treated at 820 °C (for 5 s), $\text{Na}_2\text{Ca}_2\text{Si}_3\text{O}_9$ crystalline phase appeared (see Figure 6). Both angular location and peak intensities match the standard PDF 22.1455. Previous studies on sintered bioactive glasses have confirmed the apparition of the same crystalline phase [27, 28]. Clupper and Hench [29] studied the crystallinity effect in the apatite formation for bioactive glasses surfaces and they revealed that the kinetic for apatite formation decreased slightly with crystal phase of $\text{Na}_2\text{Ca}_2\text{Si}_3\text{O}_9$, but there was apatite formation in any case [30]. In vitro bioactivity was investigated by BG-coated titanium substrates by immersion in SBF for 21 days. SEM micrographs and XRD results are shown in Figure 6. After the SBF test, $\text{Na}_2\text{Ca}_2\text{Si}_3\text{O}_9$ phase disappeared, forming HA particles on both coating-substrate systems. The morphological characteristics, diffraction pattern peaks and Ca/P atomic ratio obtained, confirmed the HA formation, similar to Ca/P atomic ratio of HA in bone (1.66). Three measurements of Ca/P ratio were carried out (relative error were between 1 and 3%).

4. CONCLUSIONS

Porous c.p. Ti substrates obtained by space holder technique solves the stress shielding and ensure the mechanical requirements of cortical bone tissue. The micro-CT is an appropriate technique for evaluating the content, size and roughness of the pores. The size of the pores allows the BG infiltration and the roughness in pores walls enhances the possible osteoblast attachment. Otherwise, a new bioactive glass deposition technique has been implemented to improve the osseointegration on titanium substrates. After in vitro studies, HA formation is confirmed despite the BG coating crystallization. In summary, the coated titanium samples show a biomechanical (stiffness and yield strength) and biofunctional (ingrowth and osseointegration) equilibrium, as well as a potential use in biomedical applications (partial substitution of bone tissue).

ACKNOWLEDGMENTS

This work was supported by the Junta de Andalucía-FEDER (Spain) through the Project Ref. P12-TEP-1401 and by the Ministry of Economy and Competitiveness of the State General Administration of Spain under the grant MAT2015-71284-P. The authors would like to thank Aldo Boccaccini and Svenja Heise for their collaboration in the review and discussion of the article, as well as to the technician J. Pinto for assistance in the micromechanical tests and Dr. Paul H. Kamm for analysis support in Fig. 1 and 2.

REFERENCES

- [1] J. P. Allain, M. Echeverry, J. J. Pavón, S. Arias, K. Iniewski, S. Selimovic, Nanostructured Biointerfaces, Chapter 2 in: Nanopatterning and Nanoscale Devices for Biological Applications, Eds., CRC Press, Taylor and Francis Group, ISBN 9781466586314, Cat# K2028, 2014.
- [2] L. Kunčická, R. Kocich, T. C. Lowe, *Progress in Materials Science* 88 (2017) 232–280.
- [3] J. D. Enderle, J. D. Bronzino, Eds.; *Introduction to biomedical engineering*, 3rd ed. Amsterdam, Boston: Elsevier Ltd, Academic Press, 2012.
- [4] Y. Torres, J. A. Rodríguez, S. Arias, M. Echeverry, S. Robledo, V. Amigo, J. J. Pavón, *J. Mater. Sci.* 47-18 (2012) 6565–6576.
- [5] S. Borjas, E. J. Gil, L. Cordero, J. J. Pavón, J. A. Rodriguez-Ortiz, A. R. Boccaccini, Y. Torres, *Key Engineering Materials* 654 (2015) 189-194.
- [6] E. J. Tobin, *Advanced Drug Delivery Reviews* 112 (2017) 88–100.
- [7] J. R. Jones, *Acta Biomaterialia* 23 (2015) S53-S82.
- [8] C. García, S. Ceré, A. Durán, *Journal of Non-Crystalline Solids* 352 (2006) 3488–3495.
- [9] A. Sola, D. Bellucci, V. Cannillo, *Biotechnology Advances* 34 (2016) 504–531.
- [10] B. Arifvianto, M. A. Leeflang, J. Zhou, *Journal of the mechanical behavior of biomedical materials* 68 (2017) 144–154.
- [11] S. Lopez-Esteban, E. Saiz, S. Fujino, T. Oku, K. Suganuma, A. P. Tomsia, *Journal of the European Ceramic Society* 23 (2003) 2921–2930.
- [12] Ö. H. Andersson, G. Liu, K. H. Karlsson, L. Niemi, J. Miettinen, J. Juhanoja, *J. Mater. Sci. Mater. Med.* 1 (1990) 219–27.

- [13] S. Muñoz, J. J. Pavón, J. A. Rodríguez-Ortiz, A. Civantos, J. P. Allain, Y. Torres, Y. Materials Characterization 108 (2015) 68-78.
- [14] ASTM C373-14, Standard test method for water absorption bulk density. Apparent porosity and apparent specific gravity of fired whiteware products, 2014.
- [15] Y. Torres, J. J. Pavón, I. Nieto, J. A. Rodríguez, Metall. Mater. Trans. B Process Metall. Mater. Process. Sci. 42 (4) (2011) 891–900.
- [16] J. Banhart, Advanced tomographic methods in materials research and engineering, First ed., Oxford University Press, New York, 2008.
- [17] ISO 13314:2011, Standard for Mechanical testing of metals — ductility testing — compression test for porous and cellular metals, 2011.
- [18] W.E. Luecke, L. Ma, S.M. Graham, M.A. Adler, Repeatability and Reproducibility of Compression Strength Measurements Conducted According to ASTM E9, NIST Technical Note 1679, 2009.
- [19] ASM-International. Nondestructive evaluation and quality control. 9th ed. 1989.
- [20] J. Müller-Rochholz, Int. J. Cem. Compos. Light. Concr. 1 (2) (1979) 87–90.
- [21] K. Mader, R. Mokso, C. Raufaste, B. Dollet, S. Santucci, J. Lambert, M. Stampanoni, Colloids and Surfaces A: Physicochem. Eng. Aspects 415 (2012) 230– 238.
- [22] M. Mata, J. Alcalá, J. Mech. Phys. Solids. 52 (2004) 145–165.
- [23] W.C. Oliver, G.M. Pharr, J. Mater. Res., Vol. 19, No. 1 (2004) 3-20.
- [24] M. R. VanLandingham, J. Res. Natl. Inst. Stand. Technol. 108 (2003) 249-265.
- [25] X. Z. Yin, T. Q. Xiao, A. Nangia, S. Yang, X. L. Lu, H. Y. Li, Q. Shao, Y. He, P. York, J. W. Zhang, Scientific Reports 1-10, 2016.
- [26] E. Maire, P. J. Withers, Quantitative X-ray tomography, International Materials Reviews 59 No 1 (2014).
- [27] D. C. Clupper, J. J. Mecholsky Jr., G. P. LaTorre, D. C. Greenspan, Biomaterials 23 (2002) 2599–606.
- [28] L. Lefebvre, J. Chevalier, L. Gremillard, R. Zenati, G. Thollet, D. Bernache-Assolant, A. Govin, Acta Mater. 55 (2007) 3305–3513.
- [29] D. C. Clupper, L. L. Hench, J. Non-Crys. Solid. 318-43 (2003) 8.
- [30] Q. Z. Chen, I. D. Thompson, A. R. Boccaccini, Biomaterials 27 (2006) 2414–2425.

Table I. Microstructural and mechanical characterization of titanium substrates.

Substrate	Archimedes' Method		Image Analysis		Micro-CT		Ultrasound Test	Uniaxial Compression		Micro-hardness	
	P _T (%)	P _i (%)	P _T (%)	D _{eq} (μm)	P _T (%)	D _{eq} (μm)	E _d (GPa)	E _c (GPa)	Yield Strength (MPa)	HV0.3	HV1
Dense	2.3 ±0.1	2.1 ±0.1	1.2 ±0.2	5.5 ±0.2	-		101.2 ±0.3	95 ±1	628 ±5	377 ±39	342 ±16
Porous	45.9 ±0.2	41.0 ±0.1	48.7 ±1.9	261.5 ±9.0	40.8 ±11.4	240.3 ±6.4	22.8 ±0.2	23.1 ±1.0	118 ±14	356 ±25	152 ±28

Figure 1. Porous substrate microstructural images: a) OM of the porous substrate, b) micro-CT, c) SEM image of the specimen's surface and d) High resolution SEM image inside the pore.

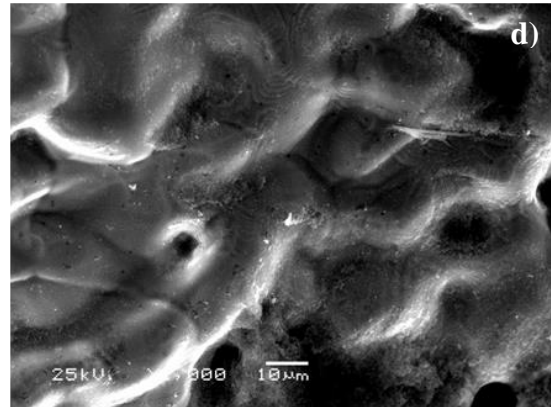
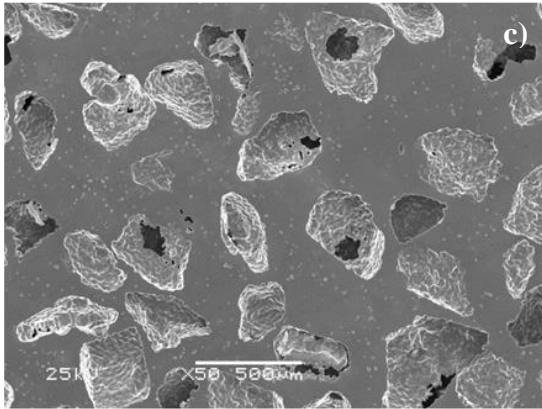
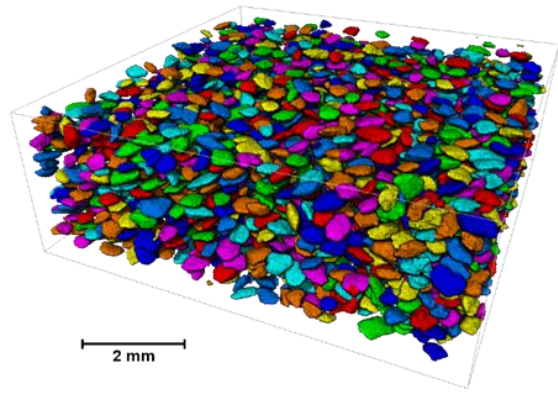
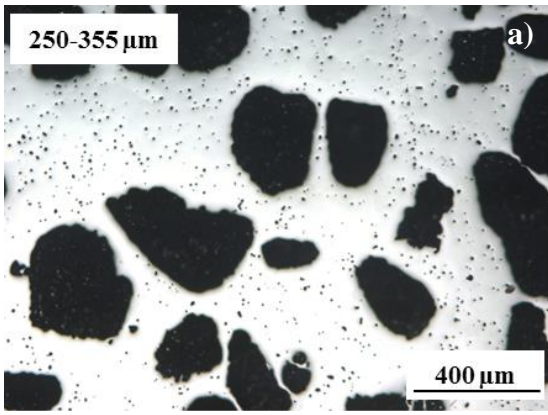
Figure 2. Morphology of the porous: a) volumetric fraction (%) vs equivalent pore diameter (μm), b) Roughness volume percentage (%), c) Roughness volume percentage (%) vs equivalent pore diameter (μm).

Figure 3. 3D macrographs of the substrates surfaces: a) full dense before TT, b) porous titanium before TT, c) full dense after TT and d) porous titanium after TT.

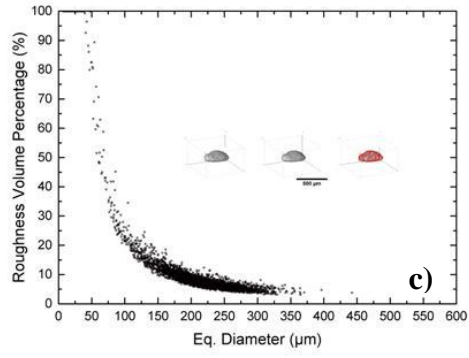
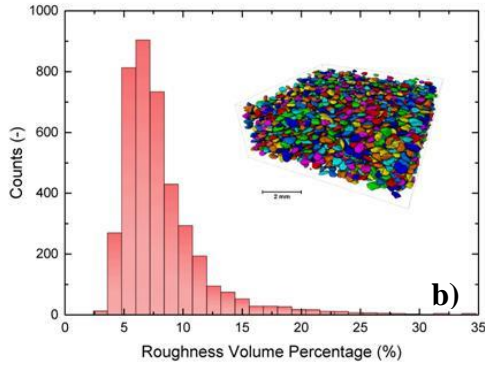
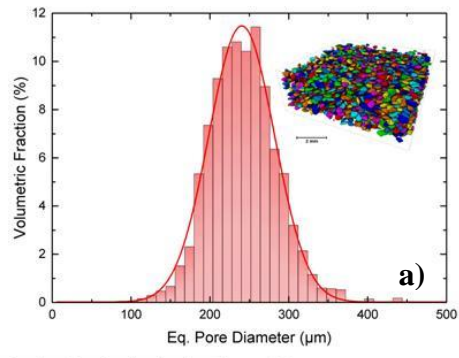
Figure 4. 3D topography of the substrates surfaces: a) full dense before coating, b) porous titanium before coating, c) full dense after coating and d) porous titanium after coating.

Figure 5. P-h curves for a dense BG pellet and BG-coated titanium substrates.





Figure 6. BG-coated titanium substrates: SEM and XRD analyses after 21 days in SBF.



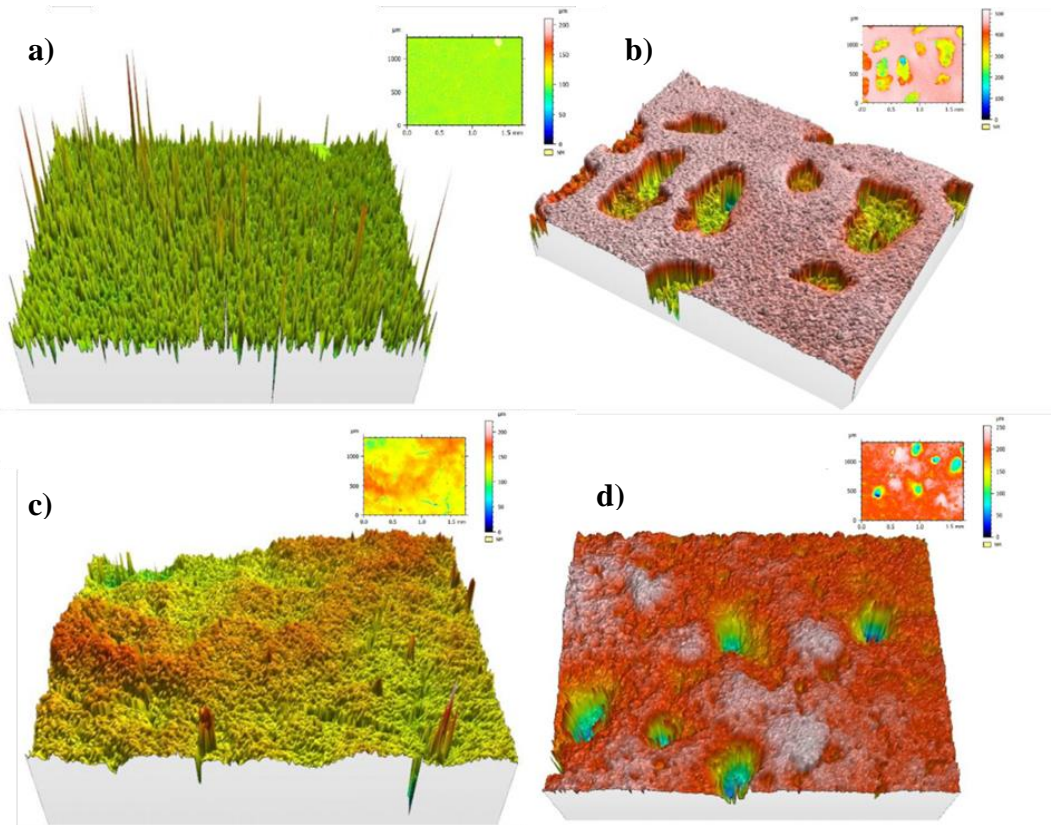
1



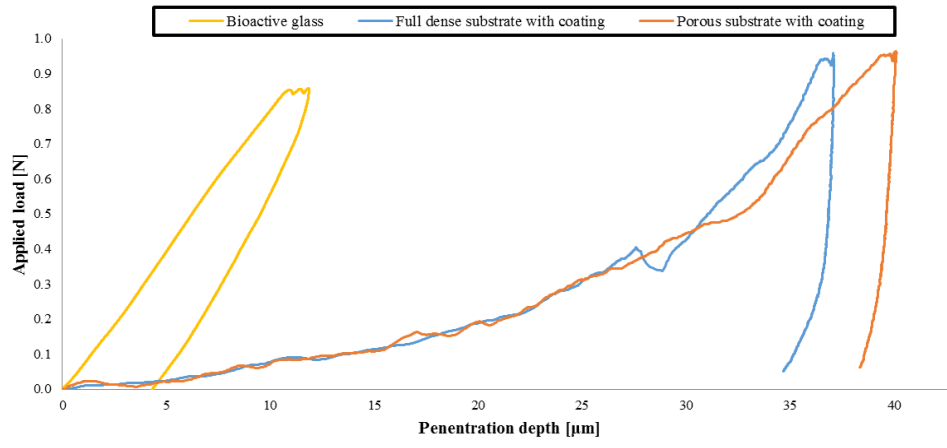
2

	Before TT	After TT
<div data-bbox="491 197 560 232" style="border: 1px solid black; padding: 2px; display: inline-block;">2 mm</div> Full dense		
250-355 μm		

3

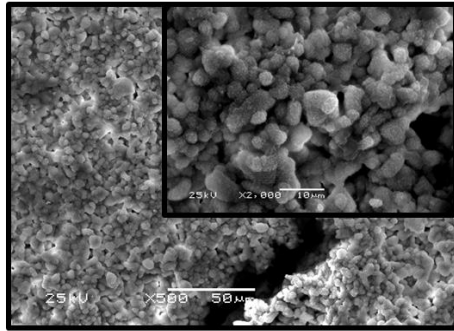


4

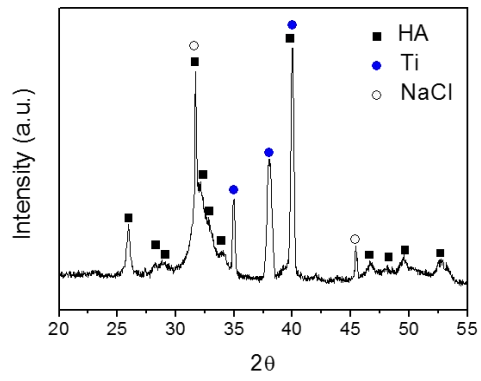


5

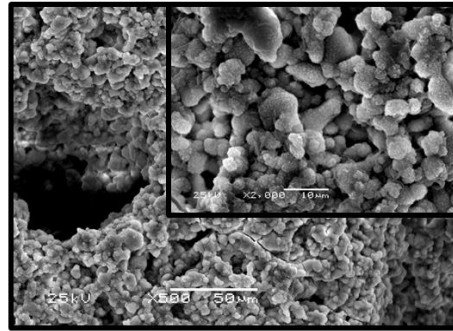
Full dense cp-Ti



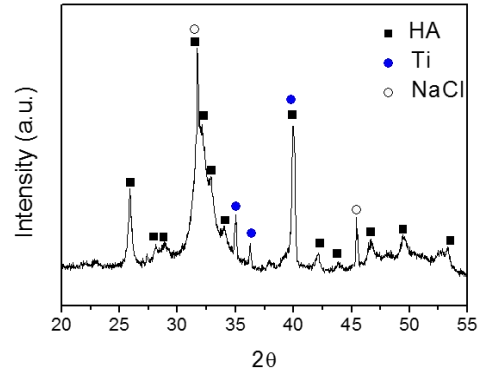
Ca/P = 1.69



cp-Ti porous



Ca/P = 1.89



6